IOP Conference Series: Materials Science and Engineering

PAPER • OPEN ACCESS

Effect of hot corrosion demeanour on aerospace-grade Hastelloy X made by pulsed and constant current arc welding in molten salts at 820 °C

To cite this article: M Sathishkumar *et al* 2020 *IOP Conf. Ser.: Mater. Sci. Eng.* **912** 032060

View the article online for updates and enhancements.

You may also like

- Ultra-thin silicate films on metals
Shamil Shaikhutdinov and Hans-Joachim Freund
- Analytical interactomic potential for a molybdenum–erbium system
Q Q Sun, T L Yang, L Yang et al.
- Size-dependent magnetism of patterned $MoTe_2$ monolayer
Yi Li, Yaqiang Ma, Zhen Feng et al.

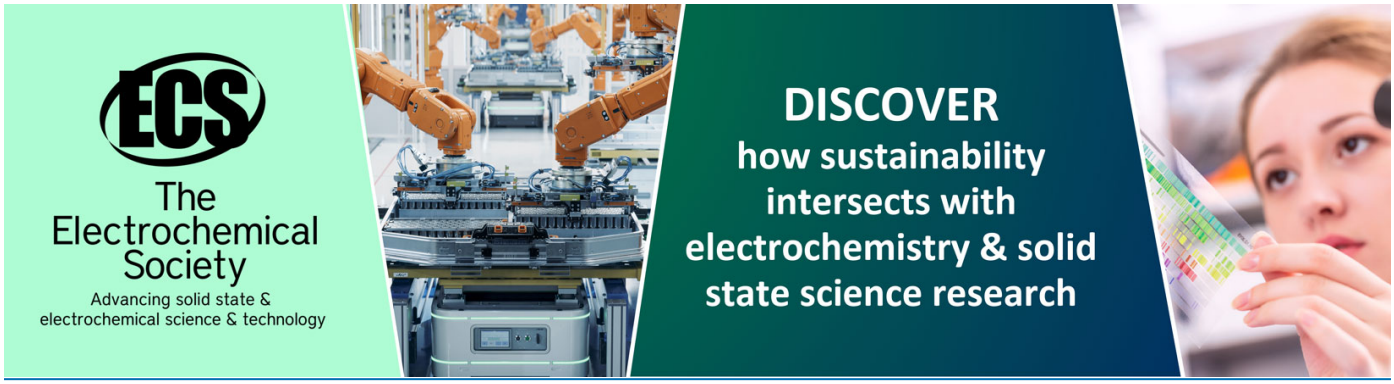

This content was downloaded from IP address 3.144.113.197 on 11/05/2024 at 08:38

IOP Conf. Series: Materials Science and Engineering **912** (2020) 032060 doi:10.1088/1757-899X/912/3/032060

Effect of hot corrosion demeanour on aerospace-grade Hastelloy X made by pulsed and constant current arc welding in molten salts at 820 °C

M Sathishkumar[1], **P Subramani**[2], **M Natesh**[1], **M Venkateshkannan**[1], **N Arivazhagan**[1], **M Manikandan**[1]
[1]School of Mechanical Engineering, Vellore Institute of Technology, Vellore, India
[2]Department of Mechanical Engineering, School of Engineering and Technology, Jain University, Bangalore, India

E-mail: desingsathish@gmail.com

Abstract. The effect of hot corrosion tendency of Hastelloy X weldment made by pulsed current tungsten inert gas (PCTIG) and constant current tungsten inert gas (CCTIG) welding has been studied. The welding has been done using ERNiCrCoMo-1 (Mo-1) filler. The hot corrosion demeanour of the Hastelloy X has studied in two different molten salt circumstance such as MS-1 (molten salt-1) ($75Na_2SO_4$ + $20V_2O_5$ + 5NaCl) and MS-2 (molten salt-2) ($75Na_2SO_4$ + $25V_2O_5$) for 25 cycles (one hour in each cycle) at 820 °C. The MS-1 substrate shows the maximum weight gain compared to MS-2. Also, the largest parabolic constant (K_p) is observed for PCTIG MS-1. The existence of NaCl in MS-1 has improved the corrosion rate by generating more spallation and exfoliation on the surface. The trends of hot corrosion resistance are following the order of, CCTIG Mo-1 MS-1 <Base Metal MS-1 <PCTIG Mo-1 MS-1 <Base Metal Mo-1 MS-2 <CCTIG MS-2 < PCTIG Mo-1 MS-2. The smaller grain size and higher protective oxides (NiO, $NiFe_2O_4$, $NiCr_2O_4$, and Cr_2O_3) developed in PCTIG MS-1 and MS-2 improves the corrosion resistance compared to coarser gains and fewer protective oxides in CCTIG MS-1 and MS-2, respectively. The non-protective oxides (Fe_2O_3 and MoO_3) improved the corrosion rate of the substrate. From this investigation, it is clear that PCTIG weldment in the MS-2 environment is providing better protection to corrosion at 820 °C.

1. Introduction

Most parts of the aerospace industry are being operated at very high temperatures. The parts used in the aerospace industries should have the ability to withstand the properties even very high temperatures. The components such as combustion cans, thrust reverser, tailpipes and afterburner are mostly made of Ni-based superalloys like Hastelloy Xwhich have the elements of Ni, Cr, Fe and Mo. Further, the oxidation resistance is being provided by Cr, and high temperature properties are mentioned with the addition of Mo and Ni [1]. The development of hot cracks over the surface of the Hastelloy X components isthe main problem which reduces the strength as well as make the components to fail at very less time. This problem can be rectified by using some kind of repairing technique like welding; instead of changing the entire parts of the combustion chamber, repairing of the components can be done [2]. This process cut down the investment for purchasing the new components. While welding again, the development of cracks over the weld bead takes place which

Content from this work may be used under the terms of the Creative Commons Attribution 3.0 licence. Any further distribution of this work must maintain attribution to the author(s) and the title of the work, journal citation and DOI.
Published under licence by IOP Publishing Ltd

can be controlled by proper selection of welding parameters. During the operating condition, these parts are exposed to the molten salt environment having a mixture of Na_2SO_4, V_2O_5,andNaCl. This causes severe corrosion on the surface. Sathishkumar and Manikandan [3]reported the reduction in the rate of hot corrosion in a molten salt environment of the weldment made by the cyclic current supply. They revealed that the cyclic current supply reduces the heat input which attributes the finer grain size and forms the protective oxides. Chellaganesh et al. [4]reported the hot corrosion demeanour of the Ni-based superalloy at 1100 °C for 50hrs. The better hot corrosion demeanour was found in the superalloy due to the presence of the spinel oxides. Salehi doolabi et al. [5] investigated the hot corrosion demeanour of Inconel 738L in a molten salt environment consist of the mixture of Na_2SO_4, V_2O_5,andNaCl. Further, they reported that the mixture with NaCl causes severe corrosion compared to the other salt. Fu guangyan et al. [6] also reported a similar increase trend of increase in hot corrosion value in NaCl environment. Sathishkumar et al. [7] also reported the welding of Hastelloy X in key-hole plasma arc welding mode. They observed the inferior results of weldment compared to the base metal. Chihiro Matsukawa et al. [8] tested the Hastelloy X material in the methane gas environment at the temperature of 800 to 1000 °C. Also, the trend of hot corrosion follows the parabolic rate.
From the above-mentioned literature, it is well known that the severe hot corrosion takes place on the surface of the components due to the deposition of Na_2SO_4, V_2O_5, andNaCl salts generated from the combustion gases. Further, the hot corrosion demeanour of the Hastelloy X welded by pulsed tungsten inert gas welding (PCTIG) at 820 °C was not investigated in severe molten salt environment consist of Na_2SO_4, V_2O_5, andNaCl. This work investigates the hot corrosion behaviour of the Hastelloy X weldment joined by pulsed current TIG (PCTIG) and continuous current TIG (CCTIG) welding, in the molten salt environment consists of MS-1 ($75Na_2SO_4 + 20V_2O_5 + 5NaCl$) and MS-2 ($75Na_2SO_4 + 25V_2O_5$)at 820 °C for 25 cycles.

2. Experimental Methodology

Solution heat-treated plate (heating:1175 °C and cooling: room temperature) has taken with the dimension of 300 × 200 × 7 mm in this study. As-received plate is cleaned with acetone and cotton to remove unwanted foreign particles. Followed by, the cleaned plate wastested to examine the elemental composition using X-ray fluorescence gun and composition is listed in Table 1. The test results were matched with the UNS N06002 as per standard (ASTM B435). The received plate having the following properties, density of 8.2 x 10^3 kg/m^3, young's modulus of 204 GPa, thermal expansion co-efficient of 13.3 x 10^6 /°C, specific heat of 459 J/Kg °C, thermal conductivity of 11.7 W/m °C, electrical resistivity of 118 x 10^{-8}, poison ratio of 0.33, and melting point of 1350 °C. Consequently, the plate was extracted in the required dimension (100 × 200 × 700 mm) using wire electrical discharge machining (WEDM). The edge of the plate has prepared with the V-groove (the bevel angle: 30°) in the milling machine. After that, the welding (butt joint) has carried out using CC-TIG and PC-TIG processes (machine: KEMPI). Table 2 provided significant process parameters. During the welding process, the groove profile has completely filled with Mo-1 filler wire. The shielding gas (Argon) with the flow rate of 15 L/min was employed to protect the molten metal completely from the atmosphere. The parameters used for computing the heat supply are voltage, mean current, arc efficiency (70%) and welding speed. Equations 1 and 2 are provided the formula required to obtain the mean current and heat supply in each pass. Subsequent to welding, the welded plates were cooled at room temperature. The radiography test has been performed to evaluate the defects in the welding and results confirmed the defect-free weldments.

Mean current,

$$I_m = \frac{(I_1 \times t_1) + (I_2 \times t_2)}{t_1 + t_2} (A) \qquad (1)$$

Heat supply in each pass,

$$HS = \eta_W \times \frac{I_m \times V}{S_w}\left(\frac{kJ}{mm}\right) \quad (2)$$

Where, η_w – Arc efficiency, I_1 – base current (A), I_2 – peak current (A), t_1 – base ON time (s), t_2 – peak ON time (s), S_w – travel speed (mm/s), V- Voltage (V), HS – heat supply (kJ/mm) and I_m – mean current. After the CCTIG and PCTIG processes, the hot corrosion samples were extracted from the welded plates in a size of 20 × 10 × 7 mm. The preparation of the two different salts such asmolten salt-1 (MS-1) ($70Na_2SO_4 + 20V_2O_5 + 5NaCl$) and molten salt-2 (MS-2) ($75Na_2SO_4 + 25V_2O_5$) were made as per real environmental conditions (combustion chamber). Before coating the molten salt on the surface of the samples, weldments of CCTIG and PCTIG were heated at a temperature of 200°C with a duration of 2 hrs to remove the moisture. Subsequently, salts were coated on the surface of the weldments by keeping the weight range of 3 mg/cm^3 to 5 mg/cm^3. After that, molten salt coated weldments were kept inside the hot tubular furnace at 820°C. After an hour, corroded samples were taken from the tubular furnace and cooled down to room temperature. Subsequently, the weight of the corroded sample was measured using the weighing machine. The macrographs of the samples were captured using the dino-lite optical macroscope. Then, the samples were kept into the furnace for the further cycle. The repetition of the aforementioned cycle was done till the 25th cycle. Subsequent to the final cycle, the proper washing with the distilled water has performed on the samples to remove the remaining salts. The morphology of the corroded samples was examined using the ZEISS EVO 18 scanning electron microscope (SEM). The elemental weight percentage of the samples were observed through the energy dispersive spectroscopy (EDS). The samples were examined through BRUKER D8 X-ray diffraction (XRD) analysis to identify the presence of the oxides and precipitates.

Table 1. Elemental composition of Hastelloy X & ERNiCrCoMo-1 in wt. %.

Elements	Elemental Composition (wt. %)	
	Hastelloy X (Base Metal)	ERNiCrCoMo-1 (Filler Material)
Ni	48.81	52.8
Cr	22.30	21.7
Fe	18.10	0.7
Mo	9.15	9.0
Al	-	1.3
Ti	-	0.3
Co	0.88	12.5
Si	0.25	0.7
Mn	0.24	0.2
W	0.20	-
C	0.05	0.6
S	0.001	0.001
P	0.02	0.001

Table 2. Welding parameters of CCTIG and PCTIG.

Parameters	CCTIG Welding	PCTIG Welding
Input current	120 Amps	120 Amps (Peak) 60 Amps (Base)
Input Voltage	11.7 V	11.1 V
Welding Travel Speed	1.3 mm/s	1.3 mm/s
Pulse Frequency	-	6 Hz
Pulse ON time	-	50 %
Argon Shielding Flow Rate	15 L/min	15 L/min
Heat Input	3 kJ/mm	2.5 kJ/mm
Arc Efficiency	70 %	70 %
Number of Passes	4	4

3. Results and Discussion

3.1 Visual Observation

The dino-lite optical microscope was used to observe the surface morphology of the weldments and base metal which are tested in the MS condition. The surface morphology of the substrates before the first cycle and after the final cycle inMS-1 and MS-2 condition is presented in figure 1 and 2 (a-f), respectively. The substrate showed clear changes in the colour during the hot corrosion process as the cycle increases. The substrates are in the light greenish colour before the first cycle. During the subsequent cycles, the colour has turned into a dark greenish colour and followed by a light grey colour in all the substrate. The changes in the colour clearly represent the occurrence of hot corrosion. Further, After the 6^{th} cycle, in most of the substrate, the spalling and chipping has occurred which improves the corrosion rate. After the final cycle, the colour of all the substrate is turned into grey colour for the CCTIG and PCTIG weldments. Also, the weld bead regions have seen clearly when compared to the base metal [3].

3.2 Corrosion Kinetic curve

The corrosion kinetic plot for the weldment made by CCTIG, PCTIG, and base metal, which are tested in the MS-1 and MS-2 conditions, are presented in figure 3 and 4. The weight gain plot has revealed that CCTIG Mo-1 MS-1 shown the highest weight gain with respect to all the remaining substrates. This high level of weight gain confirmed the severe corrosion of the CCTIG Mo-1 MS-1 substrate. Further, the salt mixture consists of NaCl (MS-1) increases the hot corrosion rate compared to the mixture without it (MS-2) [5,9]. The MS-2 substrates of both the base metal and weldment are given better protection compared to the MS-1 substrate. The rate of hot corrosion can be correlated with parabolic constant (K_p) which is evaluated from the below equation 3. The K_p values for base metal, CCTIG, PCTIG weldments in both MS-1 and MS-2 conditions are given in Table 3.

$$(\frac{\Delta W}{A})^2 = K_p \times t \qquad (3)$$

Where, A is surface area in cm^2, W is a difference in final and initial weight in mg, t is the time taken in s, K_p is the parabolic constant in $mg^2/(cm^4.s)$. From the results, it is well known that the highest K_p has observed for the CCTIG Mo-1 MS-1 whereas, the lowest value is identified for the PCTIG Mo-1 MS-2 substrate. The trends of hot corrosion resistance are following the order of, CCTIG Mo-1 MS-1 < Base Metal MS-1 < PCTIG Mo-1 MS-1 < Base Metal MS-2 < CCTIG Mo-1 MS-2 < PCTIG Mo-1 MS-2. The same kind of trend has also observed for the weight gain square plot of CCTIG, PCTIG, and base metal substrates in both MS-1 and MS-2 conditions [3,10].

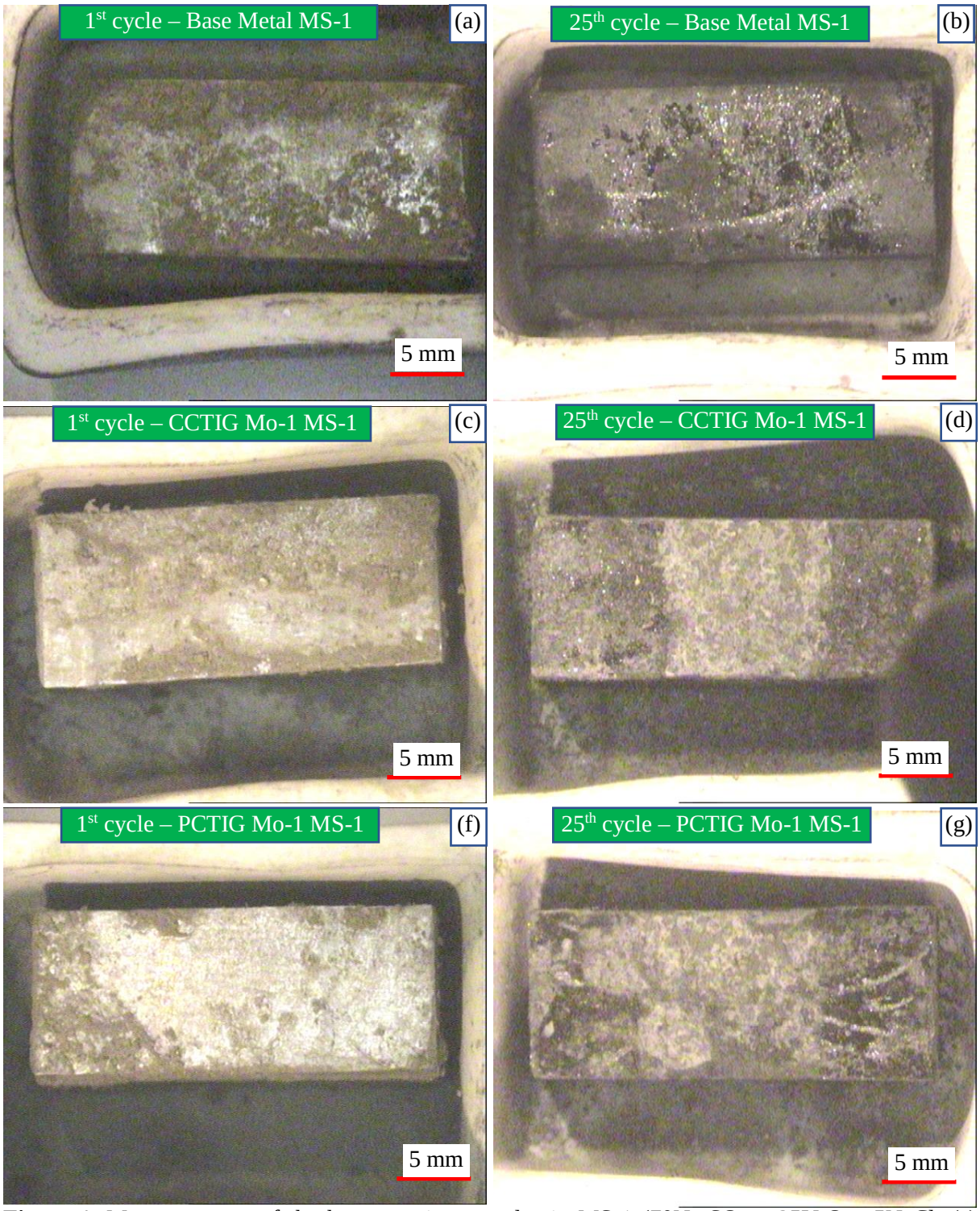

Figure 1. Macrostructure of the hot corrosion samples in MS-1 ($70Na_2SO_4$ + $25V_2O_5$+ 5NaCl; (a) Base Metal – Before 1st cycle, (b) Base Metal- After 25th cycle, (c) CCTIG Mo-1 - Before 1st cycle, (d) CCTIG Mo-1 - After 25th cycle, (e) PCTIG Mo-1 - Before 1st cycle (f) PCTIG Mo-1 - After 25th cycle.

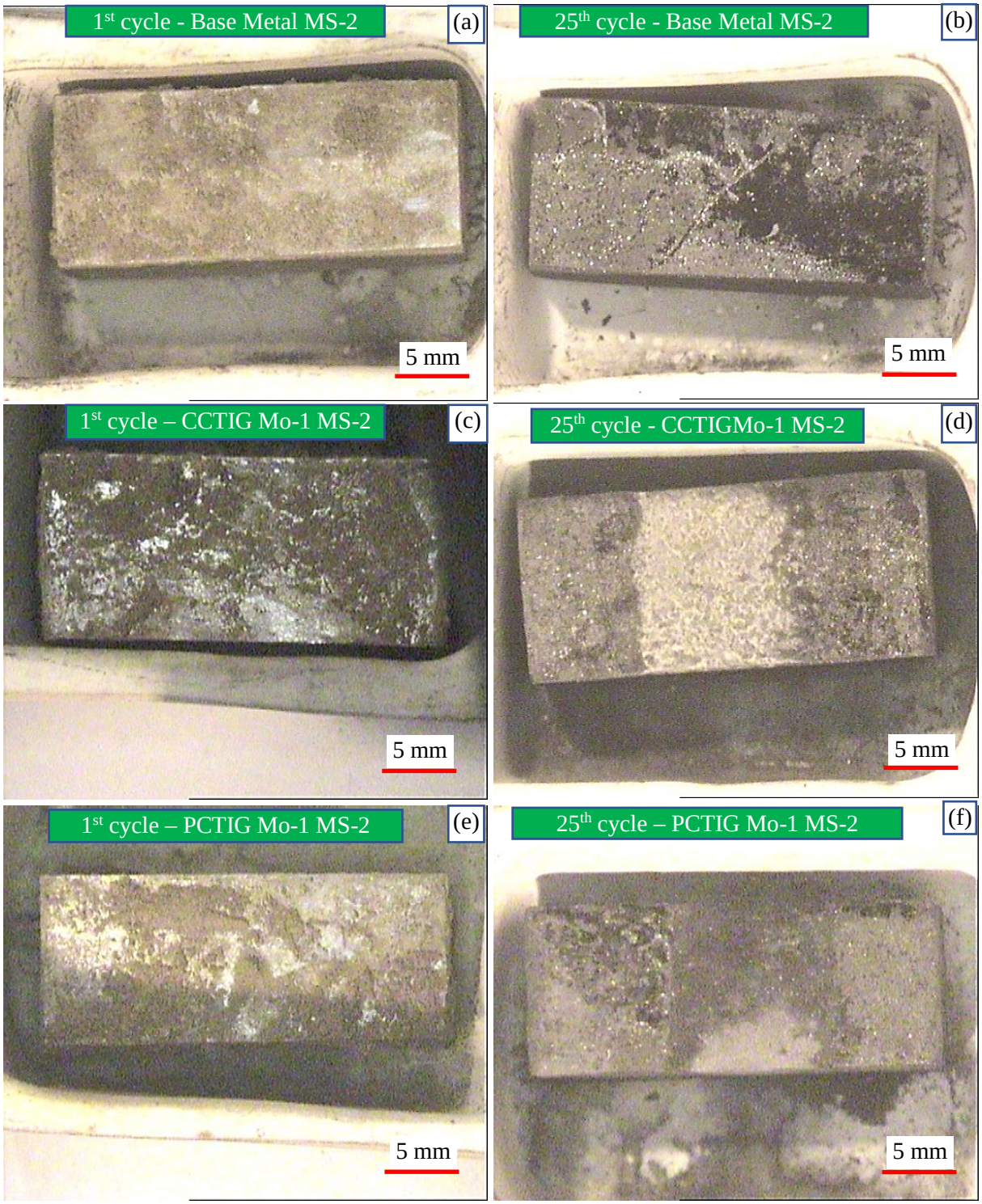

Figure 2. Macrostructure of the hot corrosion samples in MS-2 ($70Na_2SO_4 + 25V_2O_5$); (a) Base Metal – Before 1st cycle, (b) Base Metal – After 25th cycle, (c) CCTIG Mo-1 - Before 1st cycle, (d) CCTIG Mo-1 - After 25th cycle, (e) PCTIG Mo-1 - Before 1st cycle (f) PCTIG Mo-1 - After 25th cycle.

Table 3. Parabolic constant (K_p) for base metal, CCTIG, and PCTIG in MS-1 and MS-2.

Type of Molten Salt	Substrate	Surface Area (A) (cm^2)	Weight gain square $(\Delta W/A)^2$ ($mg^2/(cm^4.s)$)	Parabolic Constant K_p ($mg^2/(cm^4.s)$)
Molten Salt-1	Base Metal	8.7127	4.92	5.46×10^{-5}
	CCTIG Mo-1	9.8636	21.26	23.62×10^{-5}
	PCTIG Mo-1	9.4163	3.37	3.74×10^{-5}
Molten Salt-2	Base Metal	8.8371	2.25	2.49×10^{-5}
	CCTIG Mo-1	9.2487	1.98	2.19×10^{-5}
	PCTIG Mo-1	9.4091	0.56	0.62×10^{-5}

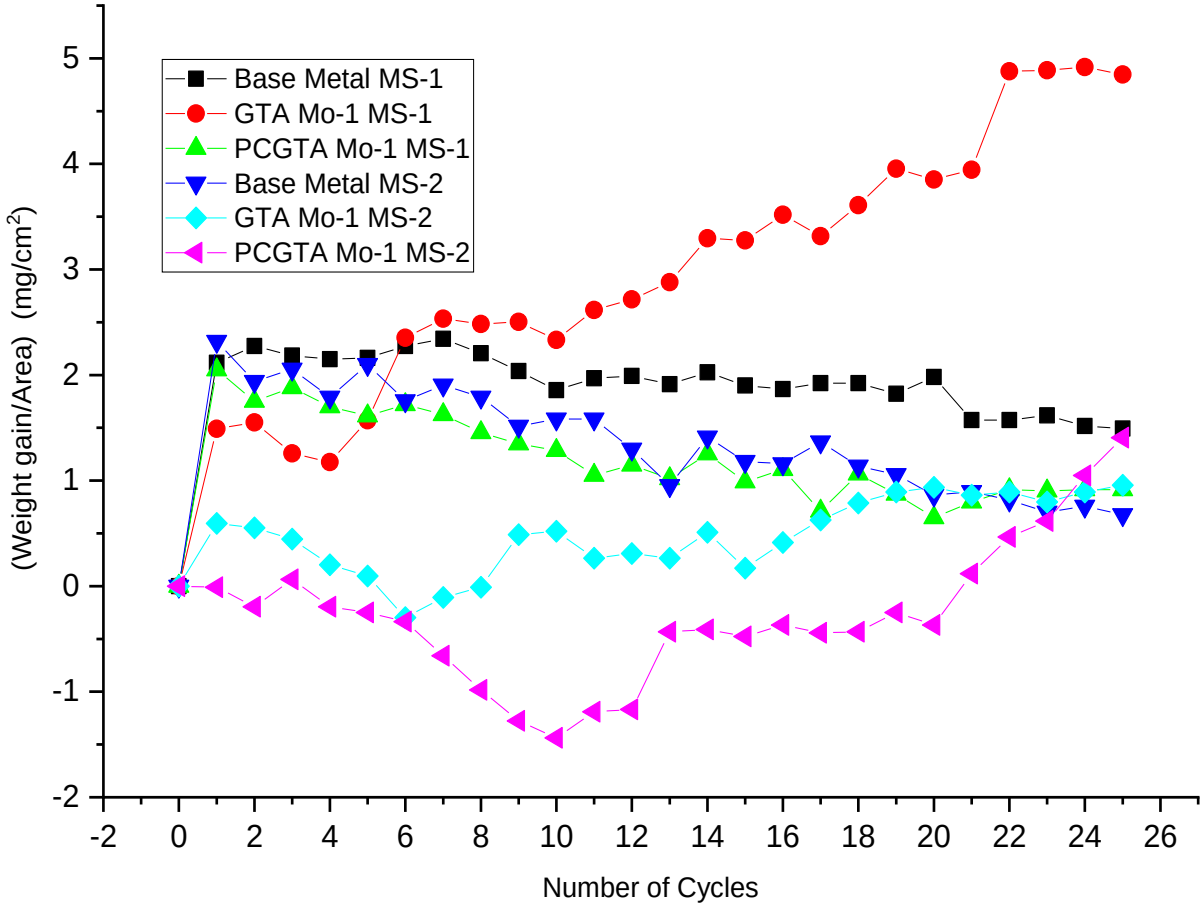

Figure 3. Hot corrosion kinetic curve of weight gain for both CCTIG Mo-1 and PCTIG Mo-1 in MS-1 & MS-2.

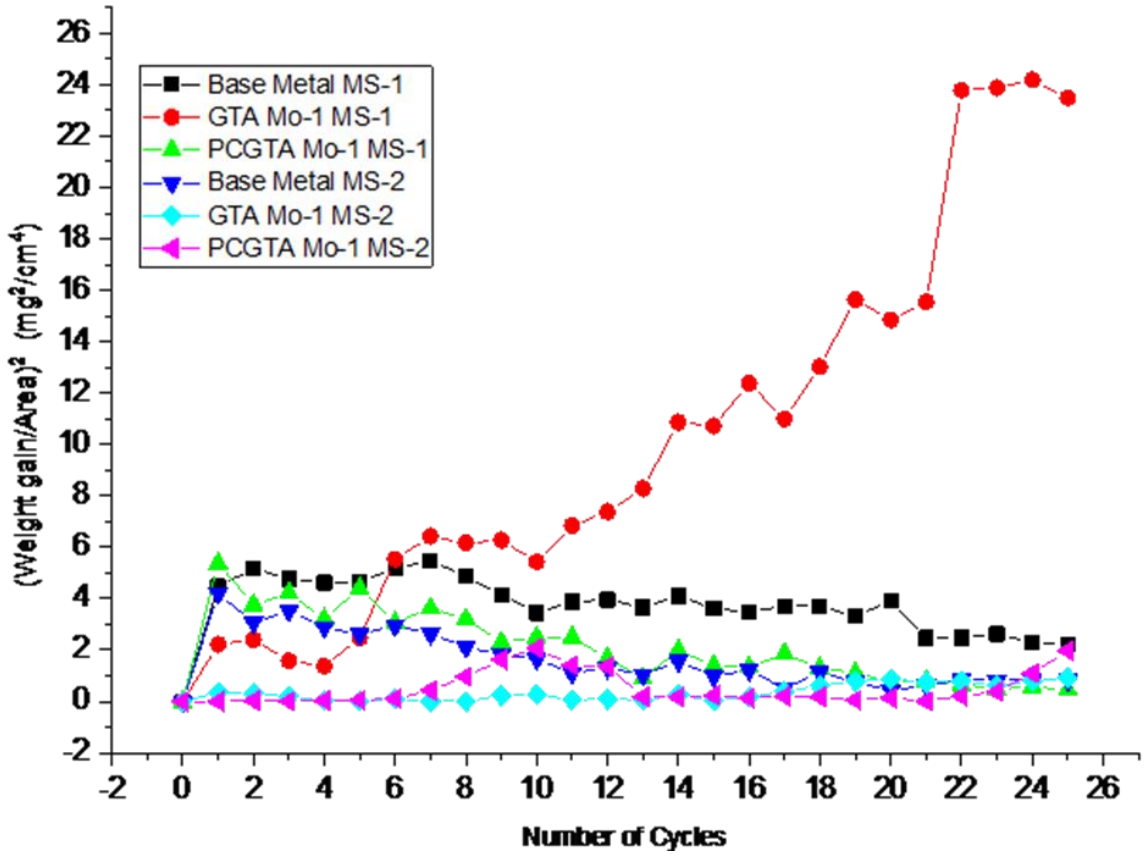

Figure 4. Hot corrosion kinetic curve of weight gain square for both CCTIG Mo-1 and PCTIG Mo-1 in MS-1 & MS-2.

3.3 SEM/EDS Analysis

The grains over the surface of the hot corrosion samples of CCTIG, PCTIG, and base metal in MS-1 and MS-2 conditions are clearly observed using the SEM photographs with a magnification of 10 k X. The substrates photograph in both MS-1 and MS-2 are presented in figure 5 and 6. It is seen from the SEM photographs that the weldments of CCTIG are shown the larger gains and grain boundary compared to the PCTIG. Also, the size of grains in the MS-2 condition is comparatively lesser than the MS-1 condition for all the weldments and base metal. The larger grain size indicated the high level of hot corrosion over the surface of the substrates. Further, the kinetic plot of MS-1 and MS-2 also revealed a similar kind of trend [6,11]. The very fine grains observed in the PCTIG Mo-1 MS-1 is attributed to low hot corrosion compared to other substrates. The EDS analysis is taken in order to confirm the kind of oxides on the surface by determining the element's weight percentage. The peaks of each elements in the EDS analysis are given in figure 5 and 6. The exact weight percentage of elements present on the CCTIG, PCTIG and base metal in both MS-1 and MS-2 conditions are given in table 4 and 5. The development of protective oxides is formed due to the existence of O, Cr, Fe and Ni over the surface of all the substrates in MS-1 and MS-2 conditions. Whereas the existence of Mo, S, V, and Fe over the surface develops the non-protective oxides. The very high level of Mo in CCTIG Mo-1 MS-1 shown a very high hot corrosion compared to others. The developed protective phases over the substrate decrease the hot corrosion rate whereas the non-protective phases are improved the hot corrosion by initiating the exfoliation, spallation, and chipping on the surface.

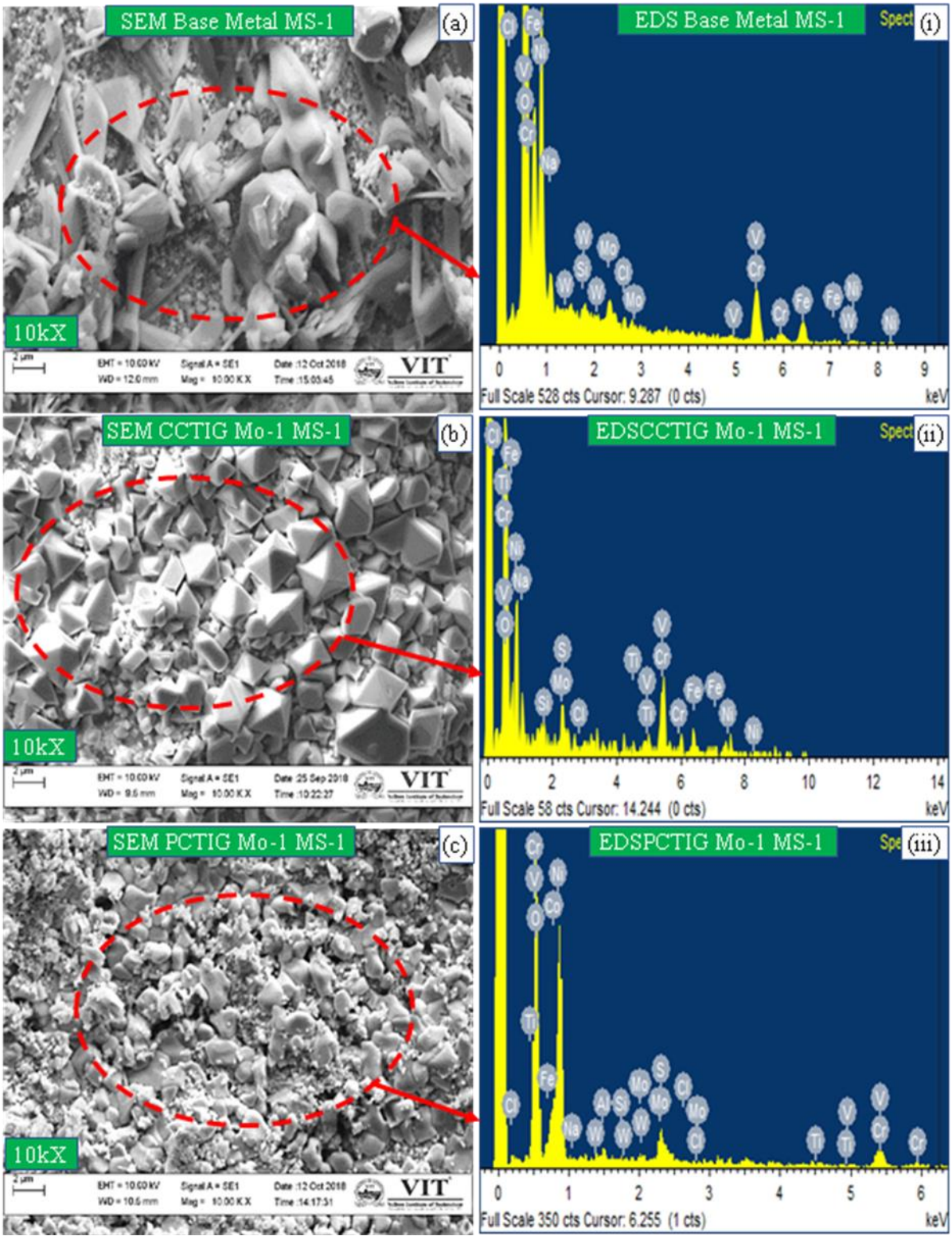

Figure 5. SEM/EDS of the hot corrosion samples in MS-1 ($70Na_2SO_4 + 25V_2O_5 + 5NaCl$); (a) SEM – Base Metal, (i) EDS – Base Metal, (b) SEM – CCTIG Mo-1, (ii) EDS – CCTIG Mo-1, (c) SEM – PCTIG Mo-1 (ii) EDS – PCTIG Mo-1.

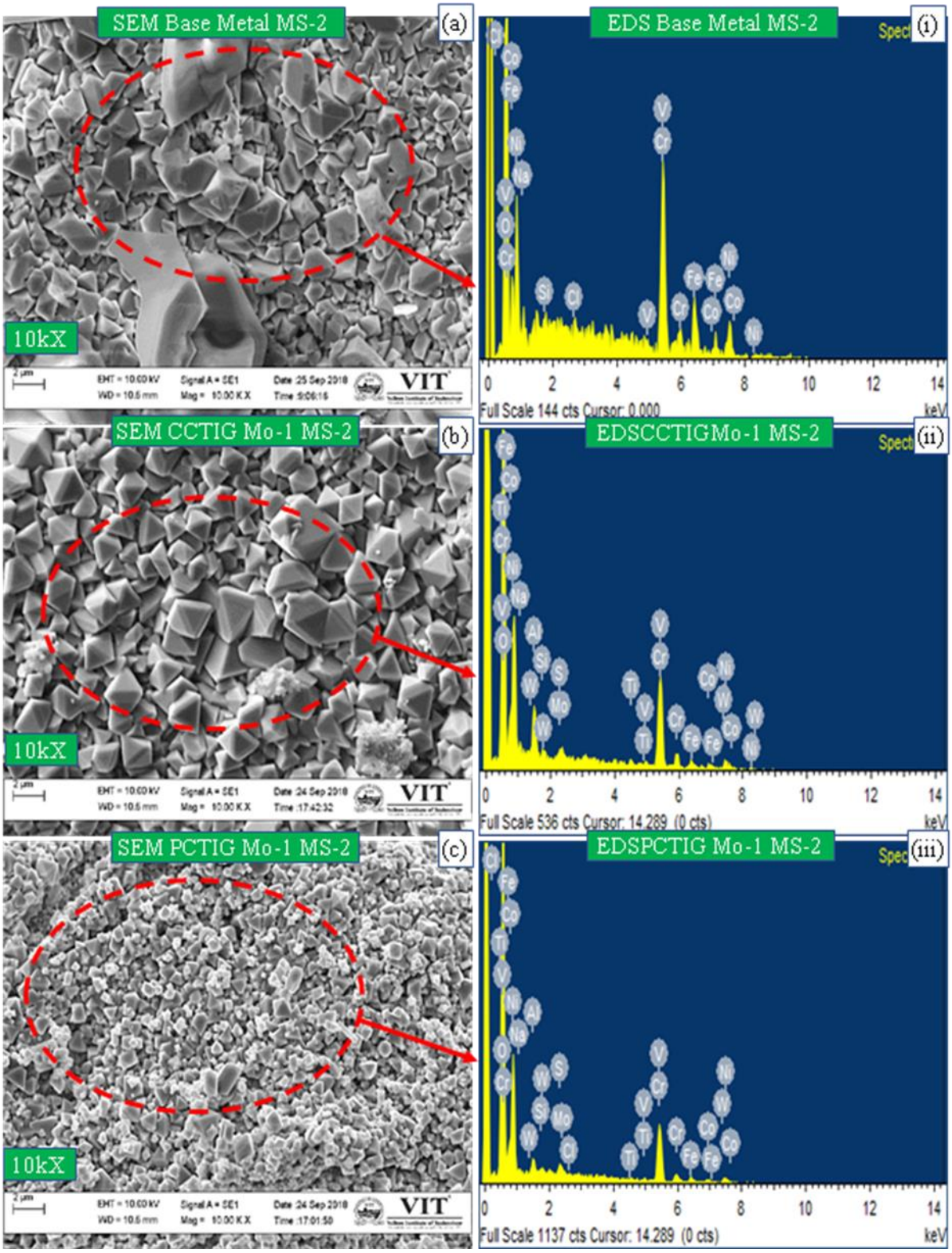

Figure 6. SEM/EDS of the hot corrosion samples in MS-2 ($75Na_2SO_4 + 25V_2O_5$); (a) SEM – Base Metal, (i) EDS – Base Metal, (b) SEM – CCTIG Mo-1, (ii) EDS – CCTIG Mo-1, (c) SEM – PCTIG Mo-1 (ii) EDS – PCTIG Mo-1.

Table 4. EDS values of base metal, CCTIG Mo-1, and PCTIG Mo-1 in MS-1 environment.

Elements	Composition (wt. %) of Base Metal in MS-1	Composition (wt. %) of CCTIG Mo-1 MS-1	Composition (wt. %) of PCTIG Mo-1 MS-1
O	24.29	27.96	25.08
Na	0.93	1.94	0.36
Al	-	0.22	0.37
Si	0.12	0.34	-
S	-	0.14	0.41
Cl	0.22	0.25	0.02
Ti	-	1.60	0.36
V	0.01	0.57	0.59
Cr	22.80	33.25	19.66
Fe	27.64	8.38	5.32
Co	-	-	3.20
Ni	22.22	20.55	42.82
Mo	1.32	4.79	1.76
W	0.43	-	0.06

Table 5. EDS values of base metal, CCTIG Mo-1, and PCTIG Mo-1 in MS-1 environment.

Elements	Composition (wt. %) of Base Metal in MS-2	Composition (wt. %) of CCTIG Mo-1 MS-2	Composition (wt. %) of PCTIGMo-1 MS-2
O	29.03	30.55	25.46
Na	5.55	0.60	0.25
Al	-	1.73	0.65
Si	0.07	0.12	0.24
S	2.96	0.42	0.34
Cl	-	0.30	0.16
Ti	-	1.58	0.38
V	0.50	0.41	0.65
Cr	22.35	32.26	38.10
Fe	19.45	4.78	5.38
Co	-	4.12	3.40
Ni	19.26	20.07	23.53
Mo	0.16	2.03	0.94
W	0.17	1.03	0.51

3.4 XRD Analysis

The presence of oxides on the substrates are identified with the help of XRD analysis. The XRD graphs of both MS-1 and MS-2 conditions are presented in figure 7.

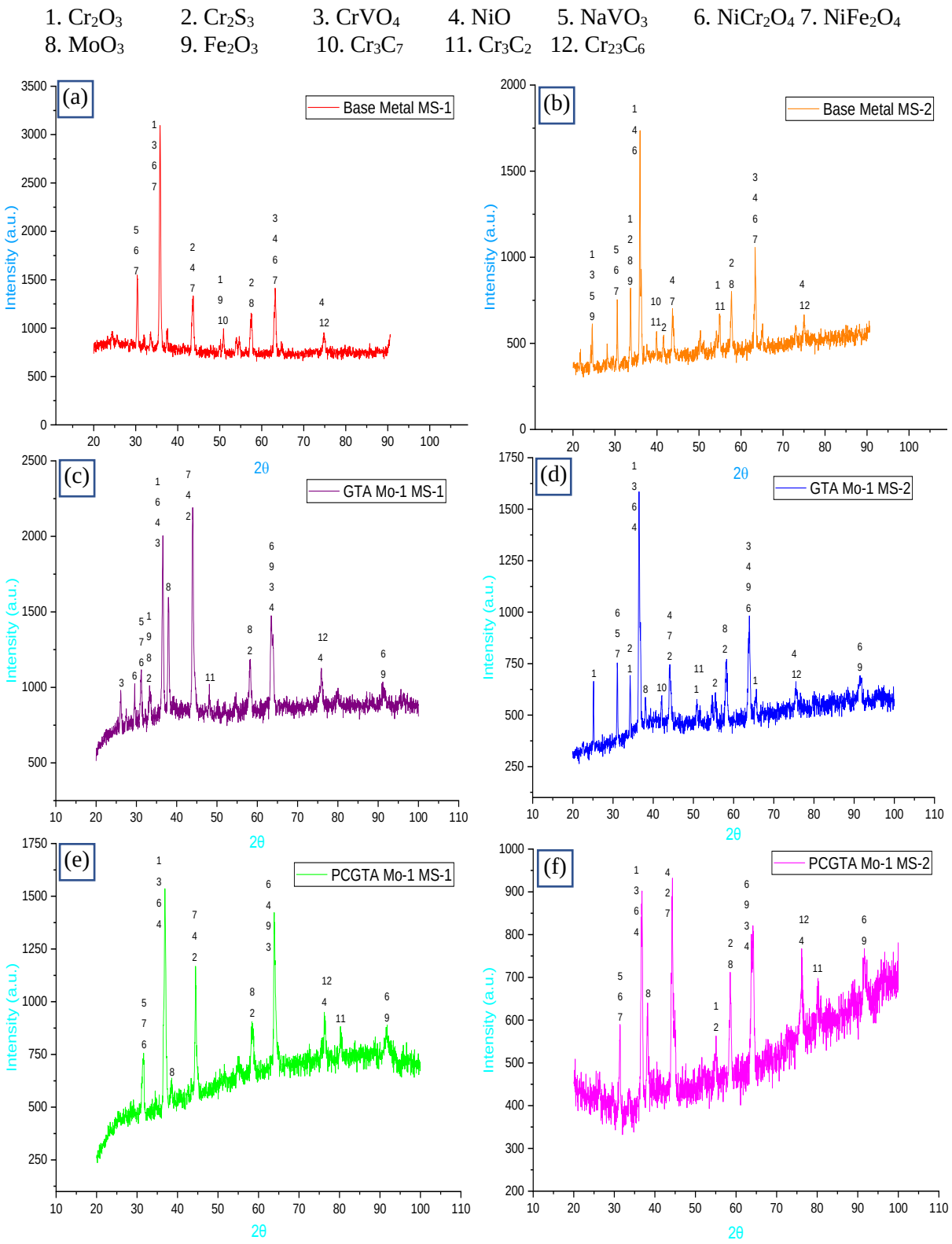

Figure 7. XRD graphs of the hot corrosion samples in MS-1 and MS-2;(a) Base Metal MS-1, (b)Base Metal MS-2, (c) CCTIG Mo-1 MS-1, (d) CCTIG Mo-1 MS-2, (e) PCTIG Mo-1 MS-1 (f) PCTIG Mo-1 MS-2.

The presence of dominant oxides like $NiFe_2O_4$, $NiCr_2O_4$, NiO, and Cr_2O_3 are identified in CCTIG Mo-1 and PCTIG Mo-1 weldments of both MS-1 and MS-2. Also, the presence of minor oxides like $NaVO_3$, $CrVO_4$, Cr_2S_3,MoO_3, and Fe_2O_3 are identified in MS-1 and MS-2 environment of both CCTIG Mo-1 and PCTIG Mo-1 have primarily attributed the exfoliation, spallation and chipping of the substrates [12]. The existence of smaller grains in PCTIG Mo-1 welding formed high-level protective oxides which prime the better hot corrosion resistance. The XRD analysis is following the same trend with SEM/EDS results. The reaction hot corrosion substrates by which the protective and non-protective oxides are formed, and it is given the below equations 4-9.

$$4Cr + 3O_2 = 2Cr_2O_3 \quad (4)$$
$$Ni + O = NiO \quad (5)$$
$$NiO + Cr_2O_3 = NiCr_2O_4 \quad (6)$$
$$NiO + Fe_2O_3 = NiFe_2O_4 \quad (7)$$
$$Na_2SO_4 + V_2O_5 = 2NaVO_3 + SO_2 + \frac{1}{2}O_2 \quad (8)$$
$$Cr_2O_3 + 2NaVO_3 = 2CrVO_4 + Na_2O \quad (9)$$

4. Conclusions

1.The Weldment joined through CCTIG, and PCTIG with Mo-1 filler are revealed defect-free weld bead.

2. The chipping and spalling improve the hot corrosion rate and it confirmed by the changes in the colour of substrates during hot corrosion tests. The colour of the substrates has changed from light greenish to dark greenish and followed by a light grey colour at the end.

3. The corrosion kinetic graphs revealed that the highest weight gain was observed for CCTIG Mo-1 MS-1, and the lowest weight gain was observed for PCTIG Mo-1 MS-1. The trends of hot corrosion resistance are following the order of, CCTIG Mo-1 MS-1 < Base Metal MS-1 < PCTIG Mo-1 MS-1 < Base Metal MS-2 < CCTIG Mo-1 MS-2 < PCTIG Mo-1 MS-2.

4. The SEM images clearly revealed that larger gains in CCTIG Mo-1 MS-1 condition, whereas the finer gains are observed in PCTIG Mo-1 MS-2. The existence of larger gains is primarily attributed to the higher hot corrosion compared to the finer gains.

5. The development of protective oxides is formed due to the existence of O, Cr, Fe and Ni over the surface of all the substrates in MS-1 and MS-2 conditions. Whereas the existence of Mo, S, V, and Fe over the surface develops the non-protective oxides. The very high level of Mo in CCTIG Mo-1 MS-1 shown a very high hot corrosion compared to others.

6. The existence of dominant oxides like $NiFe_2O_4$, $NiCr_2O_4$, NiO, and Cr_2O_3 are found in CCTIG Mo-1 and PCTIG Mo-1 weldments of both MS-1 and MS-2. Also, the presence of minor oxides like $NaVO_3$, $CrVO_4$, Cr_2S_3,MoO_3, and Fe_2O_3 are identified in MS-1 and MS-2 environment of both CCTIG Mo-1 and PCTIG Mo-1 have primarily attributed the exfoliation, spallation and chipping of the substrates.

Acknowledgement

The authors would like to thank the Vellore Institute of Technology (VIT), Vellore, for support in the purchase of Hastelloy X and studying the weldment properties by allotting the required SEED GRANT.

5. References

[1] Inconel alloy HX (UNS N06002) 2005 Technical data sheet *Special Metal Corporation* 1–8
[2] Sathishkumar M and Manikandan M 2019 Preclusion of carbide precipitates in the Hastelloy X weldment using the current pulsing *technique J. Manuf. Process.* **45** 9-21
[3] Sathishkumar M and Manikandan M 2019 Hot corrosion behaviour of continuous and pulsed current gas tungsten arc welded Hastelloy X in different molten salts environment *Materials*

Research Express **6** 126553

[4] Chellaganesh D, Khan M A and Jappes J T W 2018 Hot corrosion behaviour of nickel–iron-based superalloy in gas turbine application *Int. J. Ambient Energy* **0750** 1–5

[5] Salehi Doolabi M, Ghasemi B, Sadrnezhaad SK, Habibollahzadeh A and Jafarzadeh K 2017 Hot corrosion behavior and near-surface microstructure of a "low-temperature high-activity Cr-aluminide" coating on inconel 738LC exposed to Na2SO4 , Na2SO4 + V2O5 and Na2SO4 + V2O5 + NaCl at 900 °C *Corrosion Science* **128** 42-53

[6] Guangyan F, Zeyan Q, Jingyu C, Qun L and Yong S 2015 Hot Corrosion Behavior of Ni-Base Alloys Coated with Salt Film of 75%Na2SO4+25%NaCl at 900 °C *Rare Met. Mater. Eng.* **44** 1112–5

[7] Sathishkumar M, Naiju C D and Manikandan M 2019 Investigation of Metallurgical and Mechanical Properties of Hastelloy X by Key-Hole Plasma Arc Welding Process *SAE Tech* 1–5

[8] Matsukawa C, Hayashi S, Yakuwa H, Kishikawa T, Narita T and Ukai S 2011 High-temperature carburization behaviour of Hastelloy X in CH4 gas. *Corros. Sci.* **53** 3131–8

[9] Kumar S, Satapathy B, Pradhan D and Mahobia GS 2019 Effect of surface modification on the hot corrosion resistance of Inconel 718 at 700 °C *Materials Research Express* **6** 086549

[10] Manikandan M, Arivarasu M, Arivazhagan N, Puneeth T, Sivakumar N, Arul Murugan B, Sathishkumar M, and Sivalingam S 2016 High Temperature Corrosion studies on Pulsed Current Gas Tungsten Arc Welded Alloy C-276 in Molten Salt Environment IOP Conference Series: Materials Science and Engineering **149**

[11] Li W, Liu Y, Wang Y, Han C and Tang H 2012 Hot corrosion behavior of Ni–16Cr–xAl based alloys in mixture of Na2SO4–NaCl at 600 °C *Trans. Nonferrous Met. Soc. China* **21** 2617–25

[12] Somasundaram B, Kadoli R and Ramesh M R 2016 Hot Corrosion Behaviour of HVOF Sprayed (Cr3C2–35 % NiCr) + 5 % Si Coatings in the Presence of Na2SO4–60 % V2O5 at 700 °C *Trans Indian Inst. Met.* **68** 257–68